

GenCA: A Text-conditioned Generative Model for Realistic and Drivable Codec Avatars

Keqiang Sun¹, Amin Jourabloo², Riddhish Bhalodia², Moustafa Meshry², Yu Rong²,
Zhengyu Yang², Thu Nguyen-Phuoc², Christian Haene², Jiu Xu², Sam Johnson²,
Hongsheng Li¹, Sofien Bouaziz²

¹ Chinese University of Hong Kong, ² Meta Reality Labs

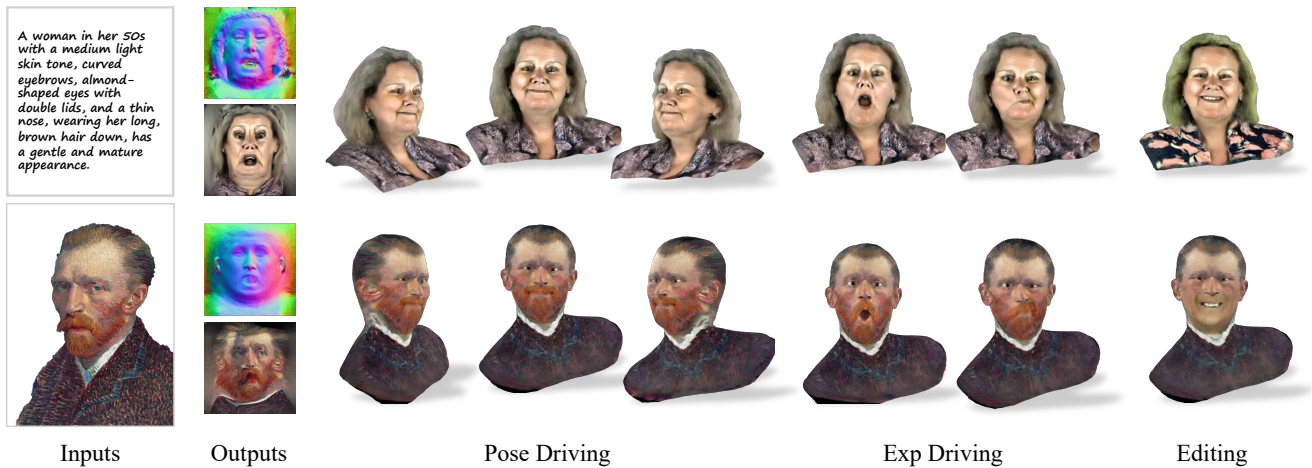


Figure 1. **Generative Codec Avatars.** Given a sentence describing the attributes of a face, our method generates a Codec Avatar, which can be driven by realistic expressions (top). GenCA has many downstream applications such as avatar reconstruction from a single in-the-wild image (bottom). Additionally, it allows for editing features, such as changing hair color to green (top) or removing facial hair (bottom).

Abstract

Photo-realistic and controllable 3D avatars are crucial for various applications such as virtual and mixed reality (VR/MR), telepresence, gaming, and film production. Traditional methods for avatar creation often involve time-consuming scanning and reconstruction processes for each avatar, which limits their scalability. Furthermore, these methods do not offer the flexibility to sample new identities or modify existing ones. On the other hand, by learning a strong prior from data, generative models provide a promising alternative to traditional reconstruction methods, easing the time constraints for both data capture and processing. Additionally, generative methods enable downstream applications beyond reconstruction, such as editing and stylization. Nonetheless, the research on generative 3D avatars is still in its infancy, and therefore current methods still have limitations such as creating static avatars,

lacking photo-realism, having incomplete facial details, or having limited drivability. To address this, we propose a text-conditioned generative model that can generate photo-realistic facial avatars of diverse identities, with more complete details like hair, eyes and mouth interior, and which can be driven through a powerful non-parametric latent expression space. Specifically, we integrate the generative and editing capabilities of latent diffusion models with a strong prior model for avatar expression driving. Our model can generate and control high-fidelity avatars, even those out-of-distribution. We also highlight its potential for downstream applications, including avatar editing and single-shot avatar reconstruction.

1. Introduction

Generating high-quality human face models has numerous applications in the gaming and film industries. Recently, social telepresence applications in virtual reality (VR) and

This work was performed during the first author’s internship at Meta, Burlingame, CA.

mixed reality (MR) have created new demands for highly-accurate and authentic avatars that can be controlled by users’ input expressions. These avatars play a vital role in improving user experience and immersion in VR and MR, making their development an area of significant interest.

Current methods for creating 3D avatars can be categorized into reconstruction-based and generative-based approaches. Reconstruction-based methods, such as the *Codec Avatar* family of works [40, 54], recover highly photo-realistic 3D avatars, but mostly rely on extensive multi-view captures of real humans. Additionally, they require a lengthy reconstruction process. Recently, [11] has reduced the need for an extensive capture by training a Universal Prior Model (UPM) using high-quality multi-view captures, and subsequently fine-tuning this learned prior with a person-specific phone scan. A state-of-the-art instant avatar method [73] made a significant stride by further relaxing the capture requirement to a monocular HD video, and reduced the avatar reconstruction time down to 10 minutes. However, these methods only reconstruct a 3D representation that replicates the identity and appearance of a given human performance capture, but support neither single-/few-shot reconstructions, nor editing capability, and cannot generate fictional avatars (*e.g.*, for the gaming and movie industries).

On the other hand, generative models, especially conditional diffusion models, have demonstrated remarkable capabilities in generating high-quality photo-realistic images from various conditional signals. These 2D image generative models can be used to generate 3D avatars [33, 66, 72] and have shown promising results for generating and *editing* high-quality avatars from text descriptions. However, the generated avatars are not photo-realistic and have limited completeness for areas such as eyes, mouth interior, hair, and wearable accessories. Moreover, to create a single avatar, these methods still rely on a lengthy optimization or distillation process even for state-of-the-art methods, such as DreamFace [72]. Other 3D generative models [12, 14, 43, 65] recover an implicit 3D representation that can be rendered from input camera views into photo-realistic images. While these methods generate photo-realistic face avatars with good completeness (*e.g.*, hair, teeth, glasses and other accessories), the generated avatars are static and cannot be driven by users’ expressions. Therefore, in this work, we combine the authenticity and drivability of Codec Avatars [11, 37], the generalization and completeness of 3D generative models [14, 65], and the intuitive text-based editing capability of 2D vision-language generative models [72] (see Table 1).

We propose Generative Codec Avatars (GenCA), a two-stage framework for generating drivable 3D avatars using only text descriptions. In the first stage, we introduce the Codec Avatar Auto-Encoder (CAAE), which learns geom-

Table 1. Comparison between our proposed method (GenCA) and state-of-the-art avatar creation methods.

	Generative	Photo-real	Completeness	Drivability	Editability
PanoHead [2]	✓	✓	✓	✗	✓
RODIN [65]	✓	✗	✓	✗	✓
ICA [10]	✗	✓	✓	✓	✗
INSTA [73]	✗	✓	✓	✓	✗
Describ3D [66]	✓	✗	✗	✓	✓
TADA [33]	✗	✗	✗	✓	✓
DreamFace [72]	✗	✓	✗	✓	✓
GenCA (ours)	✓	✓	✓	✓	✓

etry and texture latent spaces from a dataset of 3D human captures. These latent spaces model the identity distribution of avatars and are combined with an expression latent space from a Universal Prior Model (UPM) [11] to enable expression-driven, high-quality rendering of the generated identities. In the second stage, we present the Identity Generation Model. Here, the Geometry Generation module learns to generate the neutral geometry code based on the input text prompt, while the Geometry Conditioned Texture Generation Module learns to generate the neutral texture conditioned on both the geometry and the text. The generated drivable avatars capture a far more complete representation of human heads (Fig. 1-top) compared to prior state-of-the-art *generative drivable avatars* [33, 66, 72]. Additionally, our method significantly improves the driving capabilities of the generated avatars, including the ability to control areas like the eyes and tongue. Those areas are neither represented nor controlled in previous methods *generative drivable avatars*, which rely on parametric face models [6]. To demonstrate the effectiveness of our learned prior, we adapt an inversion process from [21, 70] to enable drivable avatar reconstruction from a single in-the-wild image (Fig. 1-bottom). We further demonstrate avatar editing results, beyond the training data, for both reconstructed and generated avatars (Fig. 1-last column). In summary, our contributions are:

- We present GenCA, the first text-conditioned generative model for photo-realistic, editable, and free-form drivable 3D avatar generation.
- We devise a Codec Avatar Auto-encoder to map facial images into the latent space, and the Identity Generation Model for the Codec Avatar generation.
- We showcase a variety of downstream applications enabled by GenCA model, including 3D avatar reconstruction from a single image, avatar editing and inpainting.

2. Related Works

Reconstruction or generating photo-realistic 3D face avatars is a well-studied problem in computer graphics and computer vision. Existing solutions often make trade-offs along different axes, such as avatar quality, model completeness, reconstruction/generation cost, driveability, editability, and

generative capability. Here we review landmark methods that are closely related to our work.

2.1. High-quality 3D Face Reconstruction

Quality-sensitive applications of realistic 3D avatars, such as those in the movie industry and Telepresence in AR/VR, can recover high-quality 3D models of target individuals. Expensive and complex multi-view capture systems [4, 5, 9, 17, 19, 69] are used to recover high-quality geometric and appearance information. Additionally, professional artists are employed to further clean up the recovered 3D model and improve its quality, completeness, and driveability [56, 72]. While this can achieve very high level of quality, it comes at the cost of an expensive and lengthy person-specific process.

2.2. Parametric Face Models

To enable accessible and cost-effective facial reconstruction, 3D Morphable Models (3DMM) [7] learn facial priors from a large dataset of high-quality face scans. Such facial priors are low-dimensional parametric models for facial geometry and appearance [7, 8, 31, 48]. Light-weight data capture such as a monocular camera or few-shot images are then used to supervise solving an optimization problem in the low-dimensional parameter space. However, the reduced user friction and data capture cost come at the expense of two axes – quality and completeness. First, the low-dimensional parameter space cannot represent identity-specific cues such as wrinkles and high-frequency appearance details, which are crucial for a photo-realistic representation of one’s identity. Second, learning a mesh-based facial prior is limited to representing regions that are well explained by a shared topology and simple deformation models. Therefore, such priors mainly represent the facial skin region, while missing out regions like the mouth interior, eyes and hair.

2.3. Neural Rendering

Neural Rendering [61, 62] techniques improved completeness and achieved photo-realistic quality by optimizing a neural representation and/or a rendering network to minimize the loss between renders and captured data. Implicit volumetric neural representations [45, 46] can recover and render highly photo-realistic head avatars, including difficult regions such as eyes and hair, but they mainly learn a static non-animatable representation. To recover dynamic and driveable avatars, a neural representation is learned on top of a parametric face model [20, 32, 63, 74], to allow expression transfer in the parametric expression space of the template face mesh.

In contrast to using parametric models to drive an avatar, another line of work [36, 37, 39, 54] learns a high dimensional latent expression space, jointly with a latent shape

and appearance code, and train an expression encoder to map tracked expressions to the expression latent space for driveability. Such models achieve ultra-realistic rendering under very challenging expressions, and are able to render challenging regions like eyes, teeth, tongue, mouth interior, and hair, but they learn subject-specific models and require high-quality multi-view data [69]. More recently, Cao *et al.* [11] generalized codec approaches to new subjects by learning an identity-conditioned Universal Prior Model (UPM) from high-quality captures, which can be fine-tuned for phone-scans of new subjects. However, the learned prior encodes identity information as high-dimensional multi-resolution feature maps and is not a generative model, which both limits editability and requires intricate fine-tuning strategy for personalization. In contrast, we propose a text-to-avatar generative model that still leverages the high quality, completeness, and driveability of Codec decoders [11, 39] as a rendering framework.

2.4. Generative Face Models

Generating photo-realistic fictional avatars is widely desired for many applications, such as gaming and virtual AI agents in AR/VR. Generative models trained on facial image datasets learn a strong prior and can dream up photo-realistic faces of non-existing people in 2D [27–30] and in 3D [2, 13, 14], and some works showed limited driveability of generated avatars using 3DMMs [58–60, 68]. However, in contrast to our approach, they can only render limited view angles and cannot transfer challenging expressions, for exemplifying showing tongue and mouth interior.

2.5. Text-to-3D Generation

Recent breakthroughs in visual-language models [50] and diffusion models [18, 23, 57] have significantly improved text-to-image generation [3, 51–53]. More recently, several works extend text-to-image models to generate 3D objects or scenes from text prompts by leveraging pre-trained text-to-image diffusion and optimizing 3D neural representations that minimizes the CLIP scores between multi-view 2D renderings and text prompts [24, 26, 41, 55, 71] or that employs a score distillation sampling (SDS) strategy [15, 25, 34, 49].

Described3D [66] is a concurrent work that generates driveable avatars from an input text prompt. However, in contrast to our proposal, their generated avatars are limited in terms of quality and completeness. For example, their method cannot generate challenging regions like the mouth interior, tongue, hair, head-wear or facial hair. Manual processing is required to add extra assets like hair or accessories. Additionally, Described3D is trained on synthetic data, so their results are far from photo-realistic. On the other hand, DreamFace [72] can produce much more appealing driveable avatars, but their method is not

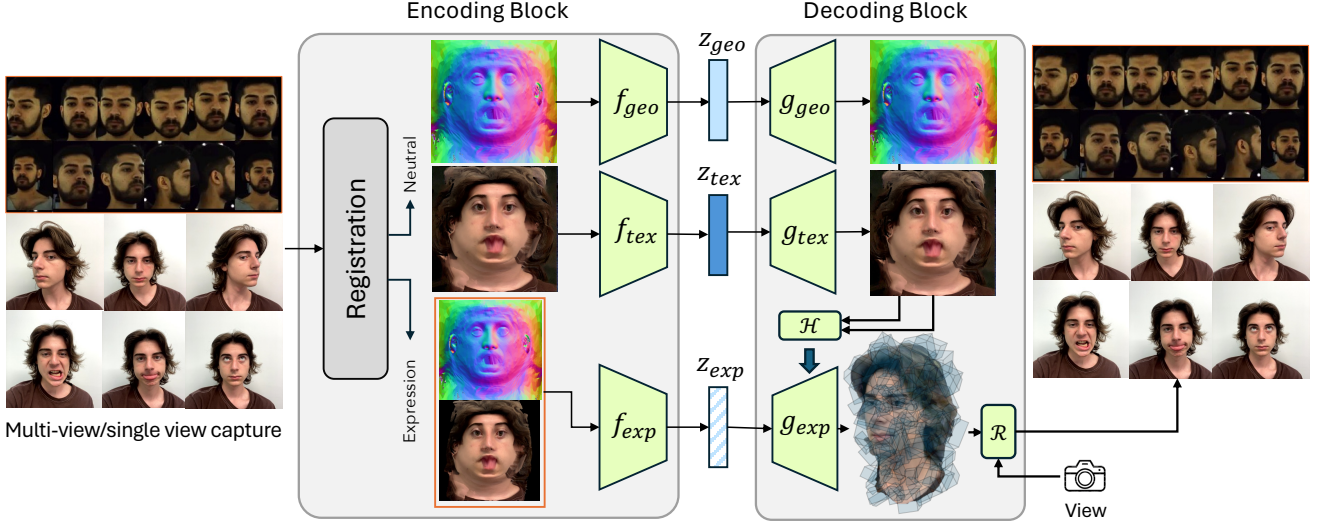


Figure 2. Main CAAE Framework for learning the latent space for geometry and texture of avatars.

a generative model. Instead, they take a compositional approach that relies on a nearest neighbor selection of a best matching geometry from a pool of acquired assets. The selected geometry is refined through an optimization process to align the avatar with the input text prompt using pre-trained Language-Vision models. And finally, a prompt-based hair selection is applied from a pool of 16 artist-created hair assets. In contrast, our method relies on a data-driven prior that learns the models photo-realistic 3D head avatars. Therefore we can generate new avatars through a simple forward pass in our model. The generated avatars are photo-realistic, driveable and achieve higher completeness compared to existing methods.

3. Methods

Given a text prompt describing \mathcal{P} the facial attributes of a random identity, GenCA generates a photo-realistic and animatable 3D avatar that matches the text prompt. To achieve this, we propose a two-stage framework for GenCA.

In the first stage (Figure 2), we introduce a Codec Avatar Auto-Encoder (CAAE) framework. The CAAE uses an *Encoding Block*, \mathcal{E} , to map input images into a factorized latent space for identity and expression. The identity latent space further broken into two latent spaces (z_{geo} , z_{tex}) for the neutral geometry and texture of any given identity. Then a *Decoding Block*, \mathcal{D} , transforms these latent codes back into realistic images.

In the second stage (Figure 3), we train an *Identity Generation Model* to learn a mapping from an input text prompt, describing an identity, to its corresponding identity latent codes (z_{geo} , z_{tex}).

During inference, given a text description of facial at-

tributes, GenCA utilizes the Identity Generation Model to sample an identity latent code and employs the Decoding Block \mathcal{D} to convert both the identity and expression codes into a photo-realistic drivable 3D avatar.

3.1. Codec Avatar Auto-Encoder (CAAE)

3.1.1 Preliminaries

Our CAAE extends the Universal Prior Model (UPM) for 3D faces proposed by [11] (Figure 2). The UPM is composed of an expression encoder f_{exp} , an identity-conditioned expression decoder g_{exp} , and a hyper-network \mathcal{H} . The expression encoder f_{exp} takes as input per-frame geometry and texture (\mathcal{G}_{exp} , \mathcal{T}_{exp}) and generates a universal expression code z_{exp} that is shared across identities. The hyper-network \mathcal{H} extracts identity features from the average neutral geometry and texture (\mathcal{G}_{neu} , \mathcal{T}_{neu}) and modulates the weights of the expression decoder g_{exp} . The expression decoder g_{exp} then decodes the expression code z_{exp} into neural volumetric primitives [37] that are rendered from any camera pose \mathcal{C} into photo-realistic images \hat{I} using a renderer \mathcal{R} .

$$\hat{I} = \mathcal{R}(g_{exp}(z_{exp} | \mathcal{H}(\mathcal{T}_{neu}, \mathcal{G}_{neu})), \mathcal{C}), \quad z_{exp} = f_{exp}(\mathcal{T}_{exp}, \mathcal{G}_{exp}) \quad (1)$$

While [11] train the UPM solely on a few hundreds of high-quality multi-view dome captures, we opt to re-train the UPM by including an additional large-scale dataset of phone captures that follow the phone scan process proposed in [11]. To bridge the domain gap between the high-quality multi-view dome captures and the simple phone captures, we apply a discriminator on the expression codes z_{exp} to encourage a unified latent space for both datasets. This additional data injection improves the UPM’s generalization ability to reconstruct diverse identities. Both the phone

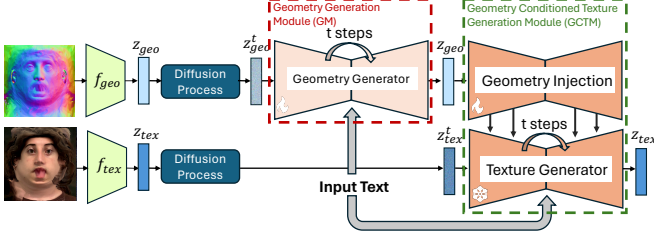


Figure 3. **Training Pipeline of the Identity Generation Model**, Geometry generator Module (GM): Generates z_{geo} of realistic geometries based on text descriptions. Geometry Conditioned Texture Generation (GCTM): Generates z_{tex} of high quality texture, consistent with conditioned geometry, based on the text descriptions.

and multi-view datasets are registered using the method proposed in [11].

We denote that the UPM from [11] is an auto-encoder framework and is not a generative model, as it neither learns avatar appearance/identity distribution, nor supports new avatar sampling. In contrast, the first stage of our GenCA (Figure 2) extends the UPM by introducing encoders and decoders for the average neutral geometry and texture (\mathcal{G}_{neu} , \mathcal{T}_{neu}), forming the Encoding and Decoding Block of our CAAE (Sec. 3.1). And the second stage of GenCA (Section 3.2) trains a generative model for the identity latent space.

3.1.2 Encoding Block

As shown Figure 2, the Encoding Block \mathcal{E} is composed of a Registration Module \mathfrak{R} , an encoder for neutral geometry UV map f_{geo} , an encoder for neutral texture UV map f_{tex} , and the expression encoder f_{exp} (introduced in Section 3.1.1).

A single or multiple input images I_{inp} of a subject is categorized into either neutral expression and expressive expression segments based on the capture script. The Registration Module \mathfrak{R} then reconstructs the per-frame geometry and the associated unwrapped texture as follows:

$$\mathcal{T}_{neu}, \mathcal{G}_{neu}, \mathcal{T}_{exp}, \mathcal{G}_{exp} = \mathfrak{R}(I_{inp}) \quad (2)$$

Specifically, it computes the average neutral geometry map \mathcal{G}_{neu} , neutral texture map \mathcal{T}_{neu} using the captured segment with neutral expression. Using the capture segment with expressive expressions, the per-frame expression geometry and texture maps \mathcal{G}_{exp} and \mathcal{T}_{exp} , as well as the camera view \mathcal{C} for each frame.

After the registration step, the Encoding Block \mathcal{E} encodes \mathcal{G}_{neu} , \mathcal{T}_{neu} , \mathcal{G}_{exp} , \mathcal{T}_{exp} into the latent space:

$$z_{geo}, z_{tex}, z_{exp} = \mathcal{E}(\mathcal{T}_{neu}, \mathcal{G}_{neu}, \mathcal{T}_{exp}, \mathcal{G}_{exp}) \quad (3)$$

where z_{geo} , z_{tex} , z_{exp} are the latent codes for geometry, texture and expression respectively. In particular, the identity geometry latent code z_{geo} and the identity texture latent code z_{tex} are computed by:

$$z_{geo} = f_{geo}(\mathcal{G}_{neu}), \quad z_{tex} = f_{tex}(\mathcal{T}_{neu}) \quad (4)$$

and the expression latent code z_{exp} is obtained as described in Equation (1).

3.1.3 Decoding Block

Given a registered camera pose \mathcal{C} , the Decoding Block \mathcal{D} maps the latent codes from the Encoding Block \mathcal{E} to a rendered image:

$$\hat{I} = \mathcal{D}(z_{geo}, z_{tex}, z_{exp}, \mathcal{C}) \quad (5)$$

In particular, the Decoding Block \mathcal{D} contains a neutral texture decoder g_{tex} and a neutral geometry decoder g_{geo} , which take the neutral geometry and texture latent codes and reconstruct the associated registered UV maps:

$$\hat{\mathcal{T}}_{neu} = g_{tex}(z_{tex}) \quad (6)$$

$$\hat{\mathcal{G}}_{neu} = g_{geo}(z_{geo}) \quad (7)$$

The Decoding Block also contains an expression decoder g_{exp} and a hyper-network \mathcal{H} as introduced in Section 3.1.1. We employ the hyper-network \mathcal{H} to extract feature maps from the reconstructed $\hat{\mathcal{T}}_{neu}$ and $\hat{\mathcal{G}}_{neu}$, which is then used to modulate g_{exp} . The output of g_{exp} is eventually rendered into an image \hat{I} by the renderer \mathcal{R} given a registered camera pose \mathcal{C} .

$$\hat{I} = \mathcal{R}(g_{exp}(z_{exp} | \mathcal{H}(\hat{\mathcal{T}}_{neu}, \hat{\mathcal{G}}_{neu})), \mathcal{C}) \quad (8)$$

3.1.4 Loss Functions

To train the f_{exp} and g_{exp} , we first employ the loss functions \mathcal{L}_{upm} from UPM [11] as the reconstruction loss. To train the identity auto-encoders, including f_{tex} , g_{tex} , f_{geo} and g_{geo} , we further compute the \mathcal{L}_1 loss for the reconstructed geometry and texture:

$$\mathcal{L}_{geo} = |\mathcal{G}_{neu} - \hat{\mathcal{G}}_{neu}|, \quad \mathcal{L}_{tex} = |\mathcal{T}_{neu} - \hat{\mathcal{T}}_{neu}| \quad (9)$$

To regularize the latent space as a normal distribution, we also minimize the Kullback–Leibler (KL) divergence \mathcal{L}_{KL} between the learned neutral geometry and texture latent distribution and a standard Gaussian distribution.

3.2. Identity Generation Model

The Codec Avatar Auto-Encoder (CAAE) introduced in Section 3.1 maps facial images into a smooth latent space, and reconstructs the latent code into images. Following Latent Diffusion Models [52], we train a diffusion model in the identity latent space $z_{id} = \langle z_{tex}, z_{geo} \rangle$. Dubbed as the Identity Generation Model, this diffusion model maps a noise map to a latent identity code conditioned on a text prompt \mathcal{P} , which can be decoded by \mathcal{D} and rendered into high-fidelity photo-realistic images.

The Identity Generation Model comprises two primary components: the Geometry Generation Module (GM) and the Geometry Conditioned Texture Generation Module (GCTM). The schematic of the Identity Generation Model is shown in Fig. 3.

3.2.1 Geometry Generation Module (GM)

Given a text prompt \mathcal{P} and a noise map z_{geo}^t , GM ϵ_θ aims to denoise from z_{geo}^t to \hat{z}_{geo}^{t-1} . By repeating this process recursively, GM eventually yields $\hat{z}_{geo}^0 \sim f_{geo}(z_{geo} | \mathcal{G}_{neu})$, which can then be decoded by Equation (7).

For training this latent diffusion model, we follow [23, 52] to perform the diffusion process manually to construct supervision. Specifically, given a latent code \mathbf{z}_{geo} , we first add noise to the t -th time step:

$$\mathbf{z}_{geo}^t = \sqrt{\alpha_t} \mathbf{z}_{geo} + \sqrt{1 - \alpha_t} \epsilon, \quad (10)$$

The network ϵ_θ then takes the noised latent code \mathbf{z}_t and time step t to predict the noise

$$\hat{\epsilon}_{geo}^t = \epsilon_\theta(\mathbf{z}_{geo}^t, t), \quad (11)$$

Finally, we re-sample the latent code \mathbf{z}_{geo}^t with the predicted noise $\hat{\epsilon}_t$

$$\hat{\mathbf{z}}_{geo}^{t-1} = h_\eta(\mathbf{z}_{geo}^t, \hat{\epsilon}_{geo}^t). \quad (12)$$

The Equation (12) and Equation (11) are recursively solved to get an estimate $\hat{\mathbf{z}}_{geo}^0$ which can be used to produce the estimated geometry by using the VAE decoder via Equation (7)

3.2.2 Geometry Conditioned Texture Generation Module (GCTM)

Directly applying the structure of GM for texture generation results in poor convergence and severe semantic misalignment, as shown in Figure 7. Inspired by ControlNet [35], we devise a Geometry Conditioned Texture Generation Module (GCTM), where the Texture Generator ϵ_ϕ takes the geometry information from the Geometry Injection ϵ_ψ module, and generates a corresponding texture latent code.

Specifically, given a geometry latent code z_{geo} , we extract feature maps with the Geometry Injection module ϵ_ψ and inject the features to the Texture Generator ϵ_ϕ , to predict the noise in z_{tex}^t :

$$\hat{\epsilon}_{tex}^t = \epsilon_\phi(z_{tex}^t, t | \epsilon_\psi(z_{geo})) \quad (13)$$

$\hat{\epsilon}_{tex}^t$ is then used for denoising, and by repeating this process, ϵ_ϕ eventually generates \hat{z}_{tex}^0 , which can be decoded via Equation (6).

We observed that training with GCTM results in better topological alignment between texture and geometry compared to standalone texture generation.

3.2.3 Loss Functions

We follow [23] and use the latent diffusion loss for both the GM and GCTM modules:

$$\mathcal{L}_{ldm} := \mathbb{E}_{\mathcal{E}(I_{inp}), \epsilon \sim \mathcal{N}(0,1), t} [\|\epsilon^t - \hat{\epsilon}^t\|_2^2]. \quad (14)$$

3.3. Inference

After training, to generate a new avatar, we first use GM to generate a high-quality UV position map based on the text description. This map is then used as an extra condition, alongside the text prompt, to generate the corresponding texture via GCTM. Their outputs, along with a selected expression code z_{exp} , are decoded by the Decoding Block and rendered into the final avatar images.

4. Experiments

4.1. Data

For training GenCA we use images data from two different sources. The first source of data is from a capture dome setup where synchronized multi-view cameras are setup and we capture an extensive set of subjects expressions as the subject follows a pre-defined expression script. The second source of data is the 12000 phone scan data which are acquired by a single view tripod video capture using iPhone 13 of the frontal face rotating in 45 degree span while maintaining the neutral expression. Both the multi-view captures as well as single view captures are collected with mindset to covering a diverse population of identities.

Both the data sources have associated attributes, and we use a large language model API for generating descriptions, more details in Supplementary.

4.2. Implementation Details

Our implementation is built upon Latent Diffusion Model (LDM). For both the GM and GCTM, we initialize the VAE with the weights pre-trained on in-the-wild image datasets.

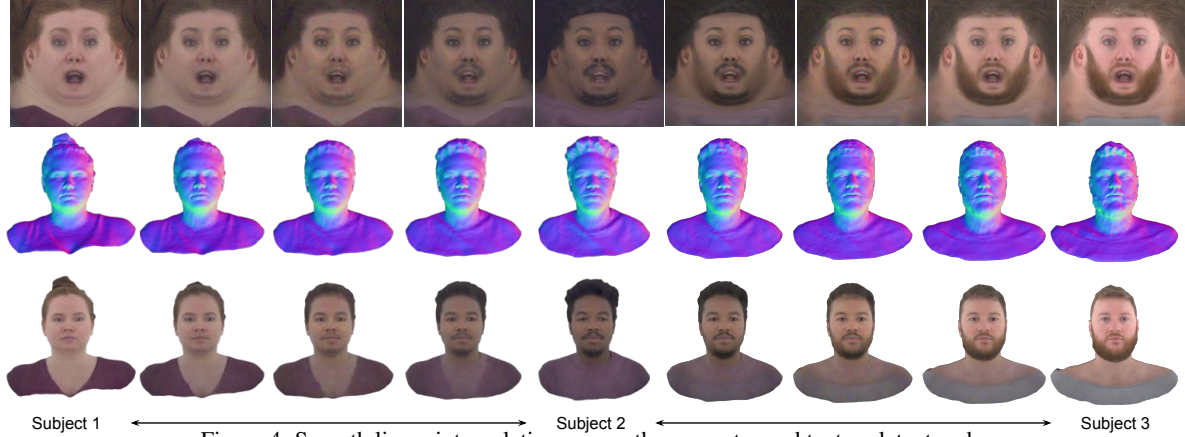


Figure 4. Smooth linear interpolation among the geometry and texture latent codes.

The AdamW optimizer with a fixed learning rate of 1×10^{-5} is employed, and the generation for geometry and texture requires 40 iterations in total. It takes about 40 seconds to generate a face on a single NVIDIA A100 GPU. We refer readers to the supplementary material for more details.

4.3. Generation Results

4.3.1 Interpolation

In Fig. 4, we show interpolation results to demonstrate the latent space of the trained CAAE can be interpolated smoothly, which lays a solid foundation for the Identity Generation Model.

4.3.2 Text conditioning generation

As shown in Fig. 5, GenCA takes a sentence in input and generate corresponding Avatars, which is faithful to the input description and can be driven to perform various wild expressions. GenCA has the capability to produce avatars with a wide range of diversity, encompassing aspects such as ethnicity, age, and appearance.

4.3.3 Additional Applications

Please note that GenCA is versatile and can be applied to various downstream tasks, such as single or multi-image registration and text-based 3D avatar editing (e.g., adjusting skin tone, goatee, clothing, hair color, etc.). Due to space constraints, the results are included in the supplementary material. We encourage you to refer to it for detailed outcomes.

4.4. Evaluation Metrics

We evaluate GenCA with several quantitative evaluation metrics common to generative models. These metrics include the contrastive language–image pretraining (CLIP) score [22], Aesthetic Score [42] and human preference

score (HPS) [67]. The CLIP score provides semantic accuracy of generation given a text caption, the Aesthetic Score evaluates the aesthetic quality of generated images and the HPS demonstrates the alignment between text-to-image generation and human preferences. In addition to these evaluation metrics we also conduct an unbiased user study.

4.5. Comparison with State-of-the-Art Methods

We compare with three state-of-the-art methods Describe3D[66], and other two SOTA methods M1 and M2 that uses generative approaches to create text-driven avatars. The qualitative comparison in Fig. 6, shows superiority of GenCA in generating photo-realistic avatars and following the text description accurately. The quantitative comparisons are shown in Table 2, GenCA performs similarly with SOTA-M2 on the CLIP score but outperforms all for the other three metrics, especially on the User Study result, GenCA achieves the best scores by a significant margin.

4.6. Ablation Study

We perform ablation studies of different components of the proposed method as shown in Fig. 7 and Table 3. For quantitative ablation, we reuse the metrics introduced in Section 4.4. We mainly explore the effects of different geometry conditioning (GeoCond) in the texture generation and the effects of the neural renderer (NeuRender). Specifically, the model without any geometry conditioning (None), as shown in the first row of Table 3 and the first column of Fig. 7, fails to learn a plausible texture, with blurry artefacts, leading to an extremely low human preference score. Taking displacement map (Disp) for geometry injection, as shown in the second row of Table 3 leads to plausible texture and significant improvement in all the metrics. However, as shown in the second column of Fig. 7, the texture is not well-aligned with the geometry, and has severe dis-



Figure 5. **Generation Results:** Qualitative results generated from the captions provided in leftmost column.

Table 2. Comparison with three state-of-the-art Methods. The three numbers for User Study denote: Semantic Alignment/Visual Appealing/Overall Preference

Method	CLIP Score	Aesthetic Score	HPS v2	User Study
Describe3D [66]	17.71	4.581	0.1510	0.61% / 7.88% / 4.85%
SOTA-M1	17.70	4.720	0.1605	2.42% / 7.27% / 6.06%
SOTA-M2	17.83	4.471	0.1635	32.73% / 1.21% / 6.06%
Ours	17.82	4.799	0.1731	64.24% / 83.64% / 83.03%

Table 3. Ablation study of the proposed method.

Condition	NeuRender	CLIP Score	Aes. Score	HPS v2
1 None	Y	17.02	4.462	0.1073
2 Disp	Y	17.45	4.737	0.1675
3 Norm	Y	17.82	4.799	0.1731
4 Norm	N	16.78	4.682	0.1530

tortion in the face. In our final design (Norm), we propose to compute the normal map as the geometry conditioning, which leads to the best performance both qualitatively and quantitatively.

Furthermore, we evaluate the effectiveness of our neural renderer with another comparison in row 3 and 4 of Table 3 and column 3 and 4 of Fig. 7. Even with the same geometry and texture map generated by our GenCA, using a traditional graphics-based renderer [47] leads to unrealistic artifacts in the skin, whereas the proposed neural rendering block yields visually appealing effects.

5. Conclusion

We propose GenCA, a text-guided generative model capable of producing photorealistic facial avatars with diverse identities and comprehensive features. With complete details, such as hair, eyes, and mouth interior, which can be driven through. We also showcase a variety of downstream applications enabled by GenCA, including avatar reconstruction from a single image, editing and inpainting. Finally, we achieve superior performance/quality in comparison to other state-of-the-art methods.

Appendices

A. Inference Architecture

Once trained, GenCA generates neutral texture and neutral geometry latent codes using input text prompt and random noise. Once we get the z_{geo} and z_{tex} , we pass it through the decoding block \mathcal{D} to obtain the UV maps $\hat{T}_{\text{neu}}, \hat{G}_{\text{neu}}$, which is then rendered using the expression and view parametrization:

A beautiful woman in her 30s with blue eyes, straight eyebrows, almond-shaped eyes, medium-sized lips, and a bottom-heavy lip shape, wearing a red lipstick, has a V-shaped face, medium-sized face, brown hair, long hair, straight hair texture, full hairline, and a light skin tone.



A middle-aged man with a round face, medium-sized eyes, and a straight nose, sporting a short beard, a horseshoe mustache, and thin lips, with a light skin tone, straight hair, and a full hairline.



A young Caucasian woman with dark brown eyes, straight eyebrows, and a medium-sized face, wearing her brown hair and having a full hairline, thin lips, a straight nose, and a light skin tone.



A young East Asian male with a medium light skin tone, dark brown almond-shaped eyes with double lids, straight eyebrows, and a bulbous nose.

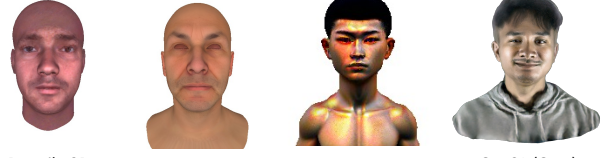


Figure 6. Qualitative comparison of GenCA generation with three state-of-the-art methods. Compared to other methods, GenCA produces more comprehensive and photorealistic avatars given the same text descriptions.

A young man in his 20s with a medium-sized, V-shaped face, dark brown eyes, and a beard. His eyes are straight and have double lids, almond-shaped and medium-sized. He has a medium-length brown hair, and a full hairline. His lips are bottom-heavy and medium-sized, and his nose is straight and medium-sized. His skin tone is light.



A young woman with dark brown eyes, straight and double-lidded, almond-shaped and medium-sized, angled and medium-thick eyebrows, an ellipse-shaped face, medium-sized and light-skinned, with a ponytail gathering long, straight brown hair, a full hairline, bottom-heavy and medium-sized lips, a straight and medium-sized nose, and a 20s age group, female gender, and no facial hair.



w/o Geometry Injector w/ Displacement Injection w/ Normal Map Injection + Differentiable Render w/ Normal Map Injection + Neural Render

Figure 7. Ablation study by disabling different parts of the proposed method.

C. Dataset

For each subject, we use a Visual Language Model (VLM) to annotate the global attributes like *age* and *gender*, and the local attributes for the *eyebrows*, *eyes*, *glasses*, *lips*, *skin tone*, *hair*, *nose*, *face shape*, *face size*, *facial hair*, *eyebrow style*, *eyebrow thickness*, *eye color*, *eye direction*, *eye lid type*, *eye shape*, *eye size*, *glasses frame*, *glasses size*, *glasses style*, *lip shape*, *lip size*, *lip stick color* etc. As an example, Fig. 8 shows the percentage distribution of both the multi-view dome dataset and the single-view phone capture with respect to three attributes (age, gender, and skintone). Eventually, we combine a Large Language Model (LLM) to summarize all these information into a sentence to describe the subject.

D. Additional Results

The Identity Generation Model with its rich identity latent space allows us to leverage the power of generative model for several applications including personalization and editing. This in turn allows for a flexible and quick way to control the avatar’s appearance while still maintaining the expression driving and generalization via the UPM.

D.1. Single/Multi-Image Personalization

Given, we have a latent space for identities we can invert into that space via the decoding block and find the z_{geo} and z_{tex} corresponding to a provided single/multi image input. More specifically, we use a single or multi-image (Fig. 11) to get an approximate UV texture and geometry, which allow us to get an initial estimate of the latent codes using the encoding block. We then leverage UPM losses ([11]) to supervise on the input data and backpropagate into the

$$\hat{I} = \mathcal{R}(g_{exp}(z_{exp} | \mathcal{H}(\hat{\mathcal{T}}_{neu}, \hat{\mathcal{G}}_{neu})), \mathcal{C}) \quad (15)$$

The inference process is shown in Figure 10

B. Additional Implementation Details

In training the Geometry Generator, we set the resolution to 1024×1024 , and set batch size to 12. We trained the Geometry Generator on use 8 NVIDIA A100 GPUs for 8 hours.

When training the Geometry-Conditioned Texture Generator, we take the ground-truth geometry map as the input condition, and the corresponding texture map as the supervision. The resolution of the Texture Generator is also set to 1024×1024 , whereas the batch size is 4, and it takes 12 hours to train on 8 NVIDIA A100 GPUs.

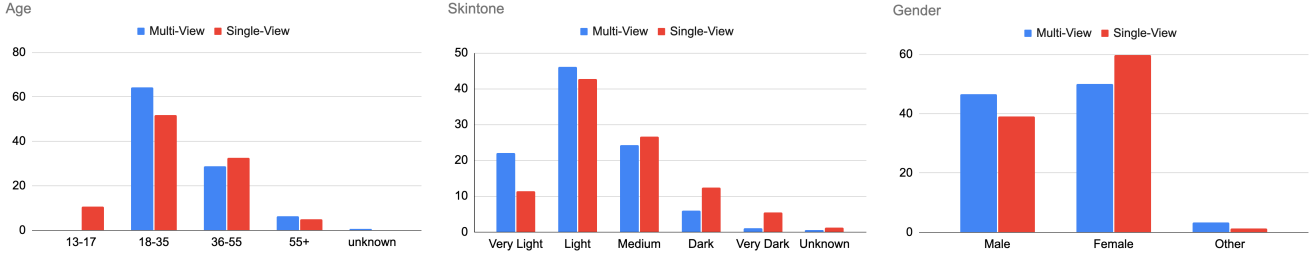
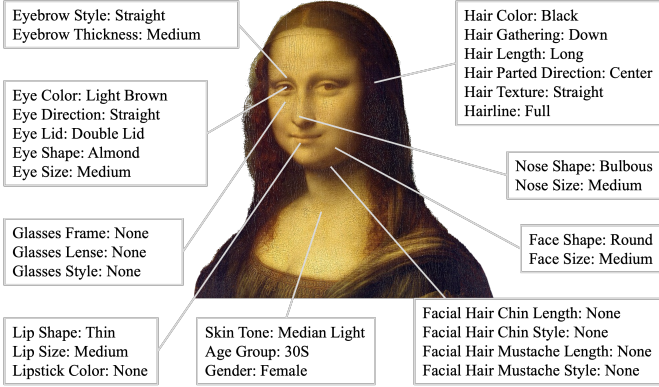


Figure 8. Data percentages with respect to three different attributes, age, skintone and gender in the multi-view and single-view captures used for GenCA training.



A female in her 30s with medium-light skin tone, medium-sized bulbous nose, thin lips, medium-sized light brown eyes with double lids, looking straight, and almond-shaped. She has medium, straight eyebrows, long, straight, black hair with a center parting, and a full hairline on a round face.

Figure 9. Example of extracting attributes and generating text caption.

identity latent space, similar methods are used for GAN inversion [1].

D.2. Editing

Given any generated or personalized avatar, we can perform global and local editing. For global appearance editing, we solely utilize text conditioning with GCTM, which alters the texture while maintaining the geometry. For local editing, we use semantic masks in the UV space to perform in-painting [38]. Specifically, given a mask M , we perform the following edit on the UV space $F_{out} = (1 - M) \times F_{edit} + M \times F_{gen}$, here F_{edit} and F_{gen} are the edited and generated geometry or texture feature respectively. This type of local editing enables us to selectively modify the avatar’s geometry (e.g., hairstyle) and texture (e.g., hair color) attributes, while leaving the rest of the avatar unchanged, as shown in Fig. 12

E. Limitation

Currently, GenCA generates texture with baked in lighting information, making it challenging to relight the generated avatars with new lighting conditions. Additionally,

our model still struggles with generating fine-grained details for regions such as hair or sharp details for the clothing regions. Finally, as our model is based on the Codec Avatar Cao et al. [11], it inherits some of its limitations, including the inability to model complex accessories like glasses or intricate and longer hairstyles.

F. Ethical Concerns and Social Impact

GenCA introduces a powerful method for generating plausible and photo-realistic 3D avatars based on text prompts, with the ability to control both view and expression. While GenCA has proven to be beneficial for many downstream tasks, it also raises significant ethical concerns, particularly regarding potential misuse.

One major risk is the possibility of personification, where the generated avatars could be used to impersonate real individuals in a misleading or harmful way. Although our method does not offer indistinguishable, pixel-perfect 2D video synthesis and does not model several critical parameters such as lighting and background—key elements typically exploited in malicious impersonation—these limitations do not entirely eliminate the risk.

To mitigate these concerns, we have implemented strict ethical guidelines in the development and deployment of GenCA. The model has been trained exclusively on data collected with prior approval, ensuring that only consenting subjects were involved in our research. Moreover, our method is intended solely for legitimate uses, such as in creative industries and virtual communication, and we strongly discourage any application that could lead to ethical violations or harm to individuals.

Equally important is the advancement of methods to detect fake content. Recent works such as [16, 44, 64] have addressed the challenge of distinguishing real from fake images. Notably, the work by Davide et al.[16] demonstrates that a CLIP-based detector, trained on only a handful of example images from a single generative model, exhibits impressive generalization abilities and robustness across different architectures, including recent commercial tools such as DALL-E 3, Midjourney v5, and Firefly.

As generative models continue to improve and access to these models becomes increasingly widespread, ongoing in-

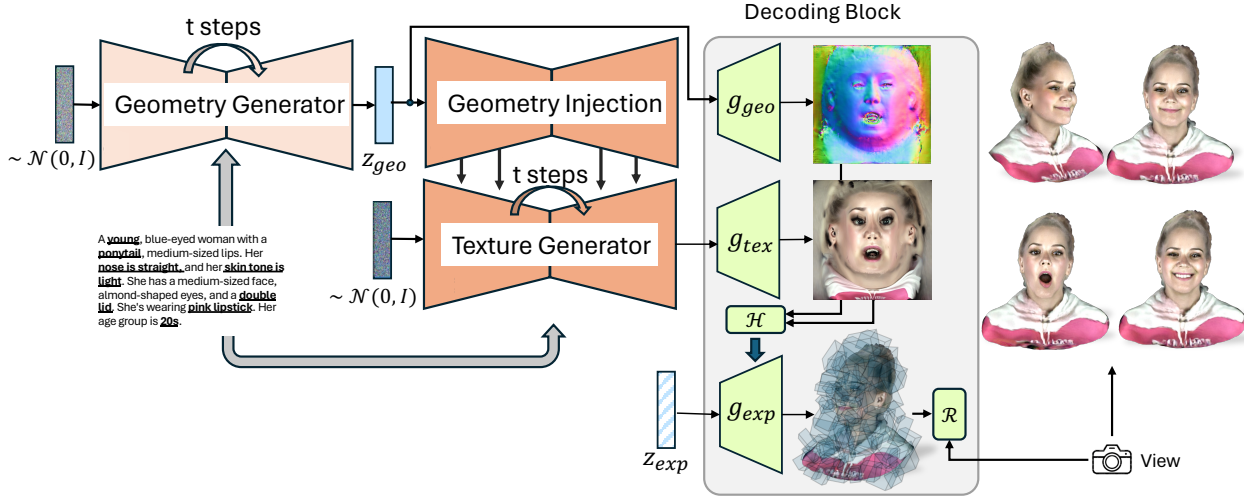


Figure 10. Inference for the GenCA. We pass in random noise and a text prompt to generate the geometry and texture neutral codes. This is then passed through the decoding block or obtaining view and expression parametrized renderings of the generated avatar.



Figure 11. Given the input image in the first column, we perform inversion to reconstruct the full Codec Avatar (second column), which can be driven with different expressions and rendered from different poses.

novation in detection methods will be essential. It is crucial to continue research in the field of fake image detection to keep pace with the rapidly evolving domain of image synthesis. Our model, GenCA, could potentially contribute to detecting fake content by providing realistic generated images and videos to enhance detection models.

References

- [1] Rameen Abdal, Yipeng Qin, and Peter Wonka. Image2stylegan: How to embed images into the stylegan latent space? In *Proceedings of the IEEE/CVF international conference on computer vision*, pages 4432–4441, 2019. 10
- [2] Sizhe An, Hongyi Xu, Yichun Shi, Guoxian Song, Umit Y Ogras, and Linjie Luo. Panohead: Geometry-aware 3d full-head synthesis in 360deg. In *Proceedings of the IEEE/CVF Conference on Computer Vision and Pattern Recognition*, pages 20950–20959, 2023. 2, 3
- [3] Yogesh Balaji, Seungjun Nah, Xun Huang, Arash Vahdat, Jiaming Song, Karsten Kreis, Miika Aittala, Timo Aila, Samuli Laine, Bryan Catanzaro, et al. ediffi: Text-to-image diffusion models with an ensemble of expert denoisers. *arXiv preprint arXiv:2211.01324*, 2022. 3
- [4] Thabo Beeler, Fabian Hahn, Derek Bradley, Bernd Bickel, Paul A Beardsley, Craig Gotsman, Robert W Sumner, and Markus H Gross. High-quality passive facial performance capture using anchor frames. *ACM Trans. Graph.*, 30(4):75, 2011. 3
- [5] Bernd Bickel, Mario Botsch, Roland Angst, Wojciech Matusik, Miguel Otaduy, Hanspeter Pfister, and Markus Gross. Multi-scale capture of facial geometry and motion. *ACM transactions on graphics (TOG)*, 26(3):33–es, 2007. 3
- [6] Volker Blanz and Thomas Vetter. A morphable model for the synthesis of 3d faces. pages 187–194, 1999. 2
- [7] Volker Blanz and Thomas Vetter. A morphable model for the synthesis of 3d faces. In *Seminal Graphics Papers: Pushing the Boundaries, Volume 2*, pages 157–164. 2023. 3
- [8] James Booth, Anastasios Roussos, Stefanos Zafeiriou, Allan Ponniah, and David Dunaway. A 3d morphable model learnt from 10,000 faces. In *Proceedings of the IEEE conference on computer vision and pattern recognition*, pages 5543–5552, 2016. 3
- [9] Derek Bradley, Wolfgang Heidrich, Tiberiu Popa, and Alla

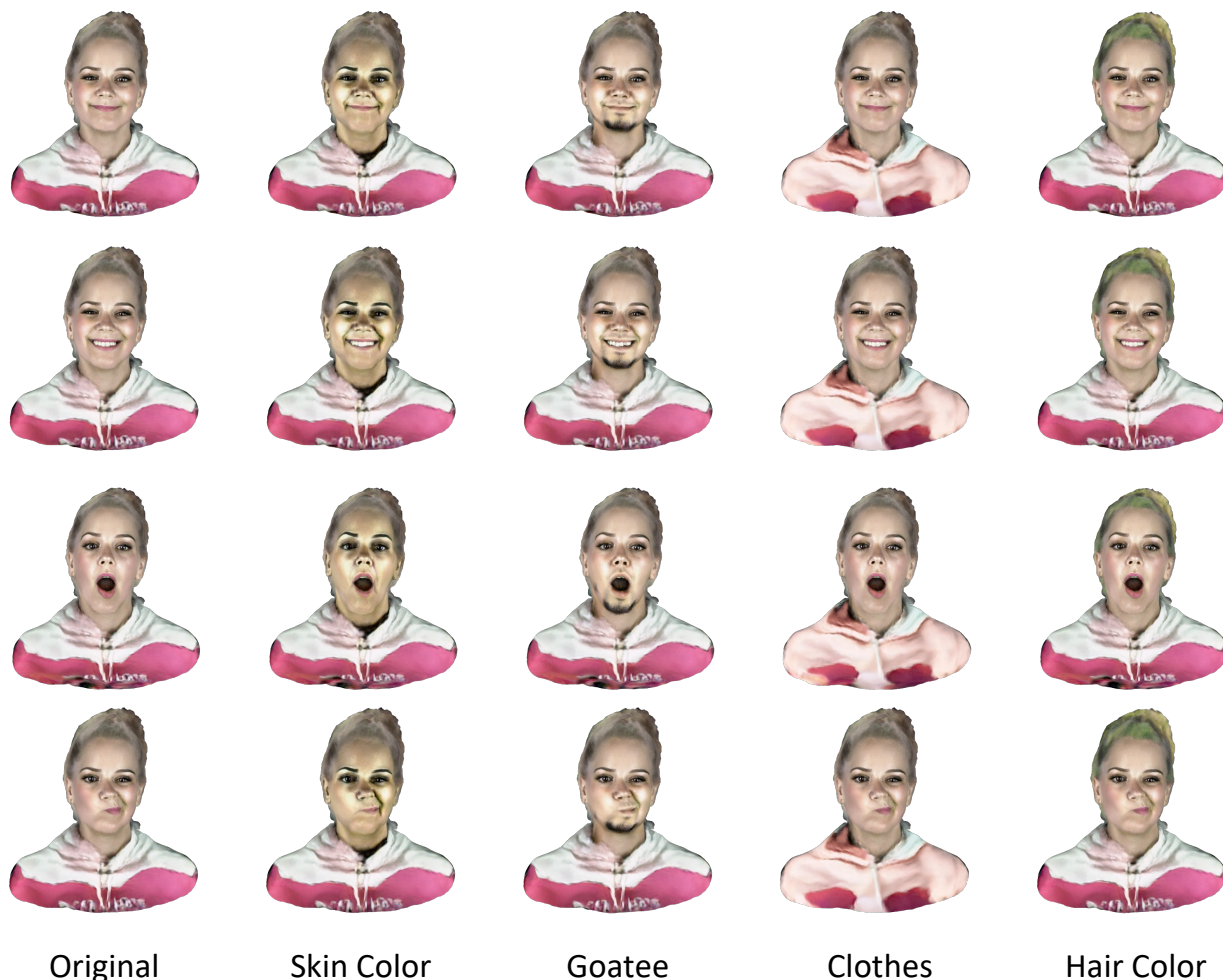


Figure 12. Editing results of generated avatar in the first column with different expressions.

- Sheffer. High resolution passive facial performance capture. In *ACM SIGGRAPH 2010 papers*, pages 1–10, 2010. [3](#)
- [10] Chen Cao, Tomas Simon, Jin Kyu Kim, Gabe Schwartz, Michael Zollhoefer, Shun-Suke Saito, Stephen Lombardi, Shih-En Wei, Danielle Belko, Shou-I Yu, Yaser Sheikh, and Jason Saragih. Authentic volumetric avatars from a phone scan. *ACM Trans. Graph.*, 41(4), 2022. [2](#)
- [11] Chen Cao, Tomas Simon, Jin Kyu Kim, Gabe Schwartz, Michael Zollhoefer, Shun-Suke Saito, Stephen Lombardi, Shih-En Wei, Danielle Belko, Shou-I Yu, et al. Authentic volumetric avatars from a phone scan. *ACM Transactions on Graphics (TOG)*, 41(4):1–19, 2022. [2](#), [3](#), [4](#), [5](#), [9](#), [10](#)
- [12] Eric R. Chan, Marco Monteiro, Petr Kellnhofer, Jiajun Wu, and Gordon Wetzstein. Pi-gan: Periodic implicit generative adversarial networks for 3d-aware image synthesis. In *Proceedings of the IEEE/CVF Conference on Computer Vision and Pattern Recognition (CVPR)*, pages 5799–5809, 2021. [2](#)
- [13] Eric R Chan, Marco Monteiro, Petr Kellnhofer, Jiajun Wu, and Gordon Wetzstein. pi-gan: Periodic implicit generative adversarial networks for 3d-aware image synthesis. In *Proceedings of the IEEE/CVF conference on computer vision and pattern recognition*, pages 5799–5809, 2021. [3](#)
- [14] Eric R Chan, Connor Z Lin, Matthew A Chan, Koki Nagano, Boxiao Pan, Shalini De Mello, Orazio Gallo, Leonidas J Guibas, Jonathan Tremblay, Sameh Khamis, et al. Efficient geometry-aware 3d generative adversarial networks. In *Proceedings of the IEEE/CVF Conference on Computer Vision and Pattern Recognition*, pages 16123–16133, 2022. [2](#), [3](#)
- [15] Rui Chen, Yongwei Chen, Ningxin Jiao, and Kui Jia. Fantasia3d: Disentangling geometry and appearance for high-quality text-to-3d content creation. *arXiv preprint arXiv:2303.13873*, 2023. [3](#)
- [16] Davide Cozzolino, Giovanni Poggi, Riccardo Corvi, Matthias Nießner, and Luisa Verdoliva. Raising the bar of ai-generated image detection with clip. In *Proceedings of the IEEE/CVF Conference on Computer Vision and Pattern Recognition*, pages 4356–4366, 2024. [10](#)
- [17] Paul Debevec, Tim Hawkins, Chris Tchou, Haarm-Pieter Duiker, Westley Sarokin, and Mark Sagar. Acquiring the reflectance field of a human face. In *Proceedings of the*

27th annual conference on Computer graphics and interactive techniques, pages 145–156, 2000. 3

- [18] Prafulla Dhariwal and Alexander Nichol. Diffusion models beat gans on image synthesis. *NeurIPS*, 34:8780–8794, 2021. 3
- [19] Graham Fyffe, Andrew Jones, Oleg Alexander, Ryosuke Ichikari, and Paul Debevec. Driving high-resolution facial scans with video performance capture. *ACM Transactions on Graphics (TOG)*, 34(1):1–14, 2014. 3
- [20] Guy Gafni, Justus Thies, Michael Zollhofer, and Matthias Nießner. Dynamic neural radiance fields for monocular 4d facial avatar reconstruction. In *Proceedings of the IEEE/CVF Conference on Computer Vision and Pattern Recognition*, pages 8649–8658, 2021. 3
- [21] Rinon Gal, Yuval Alaluf, Yuval Atzmon, Or Patashnik, Amit Haim Bermano, Gal Chechik, and Daniel Cohen-or. An image is worth one word: Personalizing text-to-image generation using textual inversion. In *The Eleventh International Conference on Learning Representations*, 2023. 2
- [22] Jack Hessel, Ari Holtzman, Maxwell Forbes, Ronan Le Bras, and Yejin Choi. Clipscore: A reference-free evaluation metric for image captioning. *arXiv preprint arXiv:2104.08718*, 2021. 7
- [23] Jonathan Ho, Ajay Jain, and Pieter Abbeel. Denoising diffusion probabilistic models. *NeurIPS*, 33:6840–6851, 2020. 3, 6
- [24] Fangzhou Hong, Mingyuan Zhang, Liang Pan, Zhongang Cai, Lei Yang, and Ziwei Liu. Avatarclip: zero-shot text-driven generation and animation of 3d avatars. *ACM TOG*, 41(4):1–19, 2022. 3
- [25] Yukun Huang, Jianan Wang, Yukai Shi, Xianbiao Qi, Zheng-Jun Zha, and Lei Zhang. Dreamtime: An improved optimization strategy for text-to-3d content creation. *arXiv preprint arXiv:2306.12422*, 2023. 3
- [26] Ajay Jain, Ben Mildenhall, Jonathan T Barron, Pieter Abbeel, and Ben Poole. Zero-shot text-guided object generation with dream fields. In *CVPR*, pages 867–876, 2022. 3
- [27] Tero Karras, Timo Aila, Samuli Laine, and Jaakko Lehtinen. Progressive growing of gans for improved quality, stability, and variation. *arXiv preprint arXiv:1710.10196*, 2017. 3
- [28] Tero Karras, Samuli Laine, and Timo Aila. A style-based generator architecture for generative adversarial networks. In *Proceedings of the IEEE/CVF conference on computer vision and pattern recognition*, pages 4401–4410, 2019.
- [29] Tero Karras, Miika Aittala, Janne Hellsten, Samuli Laine, Jaakko Lehtinen, and Timo Aila. Training generative adversarial networks with limited data. *Advances in neural information processing systems*, 33:12104–12114, 2020.
- [30] Tero Karras, Samuli Laine, Miika Aittala, Janne Hellsten, Jaakko Lehtinen, and Timo Aila. Analyzing and improving the image quality of stylegan. In *Proceedings of the IEEE/CVF conference on computer vision and pattern recognition*, pages 8110–8119, 2020. 3
- [31] Ira Kemelmacher-Shlizerman. Internet based morphable model. In *Proceedings of the IEEE international conference on computer vision*, pages 3256–3263, 2013. 3
- [32] Tobias Kirschstein, Shenhan Qian, Simon Giebenhain, Tim Walter, and Matthias Nießner. Nersemble: Multi-view radiance field reconstruction of human heads. *arXiv preprint arXiv:2305.03027*, 2023. 3
- [33] Tingting Liao, Hongwei Yi, Yuliang Xiu, Jiayang Tang, Yangyi Huang, Justus Thies, and Michael J. Black. TADA! Text to Animatable Digital Avatars. In *International Conference on 3D Vision (3DV)*, 2024. 2
- [34] Chen-Hsuan Lin, Jun Gao, Luming Tang, Towaki Takikawa, Xiaohui Zeng, Xun Huang, Karsten Kreis, Sanja Fidler, Ming-Yu Liu, and Tsung-Yi Lin. Magic3d: High-resolution text-to-3d content creation. In *CVPR*, pages 300–309, 2023. 3
- [35] Illyasviel. Controlnet. <https://huggingface.co/runwayml/lllyasviel/sd-controlnet-depth>, 2023. 6
- [36] Stephen Lombardi, Jason Saragih, Tomas Simon, and Yaser Sheikh. Deep appearance models for face rendering. *ACM Transactions on Graphics (ToG)*, 37(4):1–13, 2018. 3
- [37] Stephen Lombardi, Tomas Simon, Gabriel Schwartz, Michael Zollhofer, Yaser Sheikh, and Jason Saragih. Mixture of volumetric primitives for efficient neural rendering. *ACM Transactions on Graphics (ToG)*, 40(4):1–13, 2021. 2, 3, 4
- [38] Andreas Lugmayr, Martin Danelljan, Andres Romero, Fisher Yu, Radu Timofte, and Luc Van Gool. Repaint: Inpainting using denoising diffusion probabilistic models. In *Proceedings of the IEEE/CVF conference on computer vision and pattern recognition*, pages 11461–11471, 2022. 10
- [39] Shugao Ma, Tomas Simon, Jason Saragih, Dawei Wang, Yuecheng Li, Fernando De La Torre, and Yaser Sheikh. Pixel codec avatars. In *Proceedings of the IEEE/CVF Conference on Computer Vision and Pattern Recognition*, pages 64–73, 2021. 3
- [40] Shugao Ma, Tomas Simon, Jason Saragih, Dawei Wang, Yuecheng Li, Fernando De La Torre, and Yaser Sheikh. Pixel codec avatars. In *Proceedings of the IEEE/CVF Conference on Computer Vision and Pattern Recognition*, pages 64–73, 2021. 2
- [41] Oscar Michel, Roi Bar-On, Richard Liu, Sagie Benaim, and Rana Hanocka. Text2mesh: Text-driven neural stylization for meshes. In *CVPR*, pages 13492–13502, 2022. 3
- [42] Naila Murray, Luca Marchesotti, and Florent Perronnin. Ava: A large-scale database for aesthetic visual analysis. In *2012 IEEE conference on computer vision and pattern recognition*, pages 2408–2415. IEEE, 2012. 7
- [43] Michael Niemeyer and Andreas Geiger. Giraffe: Representing scenes as compositional generative neural feature fields. In *Proc. IEEE Conf. on Computer Vision and Pattern Recognition (CVPR)*, 2021. 2
- [44] Utkarsh Ojha, Yuheng Li, and Yong Jae Lee. Towards universal fake image detectors that generalize across generative models. In *Proceedings of the IEEE/CVF Conference on Computer Vision and Pattern Recognition*, pages 24480–24489, 2023. 10
- [45] Keunhong Park, Utkarsh Sinha, Jonathan T. Barron, Sofien Bouaziz, Dan B Goldman, Steven M. Seitz, and Ricardo

- Martin-Brualla. Nerfies: Deformable neural radiance fields. *ICCV*, 2021. 3
- [46] Keunhong Park, Utkarsh Sinha, Peter Hedman, Jonathan T. Barron, Sofien Bouaziz, Dan B Goldman, Ricardo Martin-Brualla, and Steven M. Seitz. Hypernerf: A higher-dimensional representation for topologically varying neural radiance fields. *ACM Trans. Graph.*, 40(6), 2021. 3
- [47] Adam Paszke, Sam Gross, Soumith Chintala, Gregory Chanan, Edward Yang, Zachary DeVito, Zeming Lin, Alban Desmaison, Luca Antiga, and Adam Lerer. Automatic differentiation in pytorch. 2017. 8
- [48] Stylianos Ploumpis, Evangelos Ververas, Eimear O’Sullivan, Stylianos Moschoglou, Haoyang Wang, Nick Pears, William AP Smith, Baris Gecer, and Stefanos Zafeiriou. Towards a complete 3d morphable model of the human head. *IEEE transactions on pattern analysis and machine intelligence*, 43(11):4142–4160, 2020. 3
- [49] Ben Poole, Ajay Jain, Jonathan T Barron, and Ben Mildenhall. Dreamfusion: Text-to-3d using 2d diffusion. *arXiv preprint arXiv:2209.14988*, 2022. 3
- [50] Alec Radford, Jong Wook Kim, Chris Hallacy, Aditya Ramesh, Gabriel Goh, Sandhini Agarwal, Girish Sastry, Amanda Askell, Pamela Mishkin, Jack Clark, et al. Learning transferable visual models from natural language supervision. In *International conference on machine learning*, pages 8748–8763. PMLR, 2021. 3
- [51] Aditya Ramesh, Prafulla Dhariwal, Alex Nichol, Casey Chu, and Mark Chen. Hierarchical text-conditional image generation with clip latents. *arXiv preprint arXiv:2204.06125*, 1(2):3, 2022. 3
- [52] Robin Rombach, Andreas Blattmann, Dominik Lorenz, Patrick Esser, and Björn Ommer. High-resolution image synthesis with latent diffusion models. In *CVPR*, pages 10684–10695, 2022. 6
- [53] Chitwan Saharia, William Chan, Saurabh Saxena, Lala Li, Jay Whang, Emily L Denton, Kamyar Ghasemipour, Raphael Gontijo Lopes, Burcu Karagol Ayan, Tim Salimans, et al. Photorealistic text-to-image diffusion models with deep language understanding. *NeurIPS*, 35:36479–36494, 2022. 3
- [54] Shunsuke Saito, Gabriel Schwartz, Tomas Simon, Junxuan Li, and Giljoo Nam. Relightable gaussian codec avatars. *arXiv preprint arXiv:2312.03704*, 2023. 2, 3
- [55] Aditya Sanghi, Hang Chu, Joseph G Lambourne, Ye Wang, Chin-Yi Cheng, Marco Fumero, and Kamal Rahimi Malekshan. Clip-forge: Towards zero-shot text-to-shape generation. In *CVPR*, pages 18603–18613, 2022. 3
- [56] Johannes L Schönberger. 3dscanstore. <https://www.3dscanstore.com/hd-head-scans/hd-head-models>, 2016. 3
- [57] Jiaming Song, Chenlin Meng, and Stefano Ermon. Denoising diffusion implicit models. In *International Conference on Learning Representations*, 2020. 3
- [58] Keqiang Sun, Shangzhe Wu, Zhaoyang Huang, Ning Zhang, Quan Wang, and Hongsheng Li. Controllable 3d face synthesis with conditional generative occupancy fields. In *Advances in Neural Information Processing Systems*, 2022. 3
- [59] Keqiang Sun, Shangzhe Wu, Ning Zhang, Zhaoyang Huang, Quan Wang, and Hongsheng Li. Cgof++: Controllable 3d face synthesis with conditional generative occupancy fields. *IEEE Transactions on Pattern Analysis and Machine Intelligence*, 2023.
- [60] Ayush Tewari, Mohamed Elgharib, Gaurav Bharaj, Florian Bernard, Hans-Peter Seidel, Patrick Pérez, Michael Zollhofer, and Christian Theobalt. Stylerig: Rigging stylegan for 3d control over portrait images. In *Proceedings of the IEEE/CVF Conference on Computer Vision and Pattern Recognition*, pages 6142–6151, 2020. 3
- [61] Ayush Tewari, Ohad Fried, Justus Thies, Vincent Sitzmann, Stephen Lombardi, Kalyan Sunkavalli, Ricardo Martin-Brualla, Tomas Simon, Jason Saragih, Matthias Nießner, et al. State of the art on neural rendering. In *Computer Graphics Forum*, pages 701–727. Wiley Online Library, 2020. 3
- [62] Ayush Tewari, Justus Thies, Ben Mildenhall, Pratul Srinivasan, Edgar Tretschk, Wang Yifan, Christoph Lassner, Vincent Sitzmann, Ricardo Martin-Brualla, Stephen Lombardi, et al. Advances in neural rendering. In *Computer Graphics Forum*, pages 703–735. Wiley Online Library, 2022. 3
- [63] Justus Thies, Michael Zollhöfer, and Matthias Nießner. Deferred neural rendering: Image synthesis using neural textures. *ACM Transactions on Graphics (TOG)*, 38(4):1–12, 2019. 3
- [64] Sheng-Yu Wang, Oliver Wang, Richard Zhang, Andrew Owens, and Alexei A Efros. Cnn-generated images are surprisingly easy to spot... for now. In *Proceedings of the IEEE/CVF conference on computer vision and pattern recognition*, pages 8695–8704, 2020. 10
- [65] Tengfei Wang, Bo Zhang, Ting Zhang, Shuyang Gu, Jianmin Bao, Tadas Baltrusaitis, Jingjing Shen, Dong Chen, Fang Wen, Qifeng Chen, and Baining Guo. Rodin: A generative model for sculpting 3d digital avatars using diffusion. In *Proceedings of the IEEE/CVF Conference on Computer Vision and Pattern Recognition (CVPR)*, pages 4563–4573, 2023. 2
- [66] Menghua Wu, Hao Zhu, Linjia Huang, Yiyu Zhuang, Yuanxun Lu, and Xun Cao. High-fidelity 3d face generation from natural language descriptions. In *Proceedings of the IEEE/CVF Conference on Computer Vision and Pattern Recognition*, pages 4521–4530, 2023. 2, 3, 7, 8
- [67] Xiaoshi Wu, Keqiang Sun, Feng Zhu, Rui Zhao, and Hongsheng Li. Human preference score: Better aligning text-to-image models with human preference. In *Proceedings of the IEEE/CVF International Conference on Computer Vision*, pages 2096–2105, 2023. 7
- [68] Yue Wu, Yu Deng, Jiaolong Yang, Fangyun Wei, Qifeng Chen, and Xin Tong. Anifacegan: Animatable 3d-aware face image generation for video avatars. *Advances in Neural Information Processing Systems*, 35:36188–36201, 2022. 3
- [69] Cheng-hsin Wu, Ningyuan Zheng, Scott Ardisson, Rohan Bali, Danielle Belko, Eric Brockmeyer, Lucas Evans, Timothy Godisart, Hyowon Ha, Alexander Hypes, et al. Multiface: A dataset for neural face rendering. in arxiv, 2022. 3
- [70] Weihao Xia, Yulun Zhang, Yujiu Yang, Jing-Hao Xue, Bolei Zhou, and Ming-Hsuan Yang. Gan inversion: A survey. *IEEE Transactions on Pattern Analysis and Machine Intelligence (TPAMI)*, 2022. 2

- [71] Jiale Xu, Xintao Wang, Weihao Cheng, Yan-Pei Cao, Ying Shan, Xiaohu Qie, and Shenghua Gao. Dream3d: Zero-shot text-to-3d synthesis using 3d shape prior and text-to-image diffusion models. In *CVPR*, pages 20908–20918, 2023. [3](#)
- [72] Longwen Zhang, Qiwei Qiu, Hongyang Lin, Qixuan Zhang, Cheng Shi, Wei Yang, Ye Shi, Sibe Yang, Lan Xu, and Jingyi Yu. Dreamface: Progressive generation of animatable 3d faces under text guidance, 2023. [2](#), [3](#)
- [73] Wojciech Zielonka, Timo Bolkart, and Justus Thies. Insta: Instant volumetric head avatars. In *IEEE Conference on Computer Vision and Pattern Recognition (CVPR)*, 2023. [2](#)
- [74] Wojciech Zielonka, Timo Bolkart, and Justus Thies. Instant volumetric head avatars. In *Proceedings of the IEEE/CVF Conference on Computer Vision and Pattern Recognition*, pages 4574–4584, 2023. [3](#)